ChemComm

This article is part of the

Artificial photosynthesis
web themed issue

Guest editor: Andrew Benniston

All articles in this issue will be gathered together online at
www.rsc.org/photosynthesis

ChemComm

Dynamic Article Links

Cite this: *Chem. Commun.*, 2012, **48**, 823–825

www.rsc.org/chemcomm

COMMUNICATION

Spectroscopic characterization of the key catalytic intermediate Ni–C in the O_2-tolerant [NiFe] hydrogenase I from *Aquifex aeolicus*: evidence of a weakly bound hydride†‡

Maria-Eirini Pandelia,[a] Pascale Infossi,[b] Matthias Stein,[c] Marie-Thérèse Giudici-Orticoni[b] and Wolfgang Lubitz*[a]

Received 30th September 2011, Accepted 14th November 2011
DOI: 10.1039/c1cc16109a

Ni–C in the O_2-tolerant hydrogenase I from *Aquifex aeolicus* binds a hydride weaker than that in O_2-sensitive hydrogenases. This is in line with the enhanced light-sensitivity of Ni–C, greater lability of the hydride complex and increased catalytic redox potentials relevant to bio-H_2 oxidation.

The constantly growing interest in alternative sources of energy has brought hydrogenases into the proscenium of future biotechnological applications. Hydrogenases are metalloenzymes that evolve or oxidize dihydrogen according to the reaction[1] $H_2 \rightleftharpoons 2H^+ + 2e^-$. An insight into their function and mechanism is important for their genetic and chemical engineering as well as for designing biomimetic model systems.[2] A recently discovered subclass of these enzymes has attracted interest due to their decreased O_2-sensitivity. The membrane bound [NiFe] hydrogenase (Hase I) from the hyperthermophilic bacterium *A. aeolicus* serves in an aerobic respiration pathway and the isolated enzyme alone or co-purified with its native electron acceptor cytochrome *b* retains catalytic activity under aerobic conditions.[3,4] Since Hase I is O_2-tolerant, thermostable and can be thermally activated, it is particularly suitable for biotechnological applications such as in biofuel cells.[4]

Electron paramagnetic resonance (EPR) and protein-film electrochemistry (PFE) studies have shown that the as-purified enzyme consists of only the readily activated Ni–B state,[5,6] which is spectroscopically similar to the one occurring in known anaerobic hydrogenases.[7] Thus, an analogous structure of the active site is expected. Fourier transform infrared (FTIR) studies[6] have supported a similar active site coordination with a conserved $Fe(CN)_2CO$ moiety. IR electrochemistry in solution revealed only four detectable redox states; namely Ni–B, Ni–SI_a, Ni–C and Ni–R.[6] All catalytic redox processes occur at approx. +100 mV more positive potentials than in standard anaerobic hydrogenases, whereas the central catalytic Ni–C intermediate is observed to be a more transient species.[6] The ability of Hase I to oxidize H_2 at higher redox potentials correlates with the upshift in the midpoint potentials of the three [FeS] clusters comprising the electron relay chain.[8] In all hydrogenases studied so far, only the Ni–C state ($S = 1/2$) has been shown to have the substrate bound in its active site,[9–11] emphasising its central role in the catalytic function (inset of Fig. 1). It is thus compelling to elucidate the geometrical and electronic structure of Ni–C in oxygen-tolerant hydrogenases, such as Hase I.

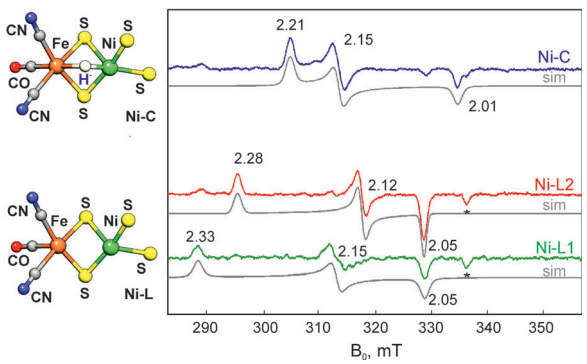

Fig. 1 CW EPR of the Hase I–cyt*b* complex in the Ni–C state at 100 K (blue). Illumination at 100 K converts Ni–C to Ni–L2 (red) and at 170 K to Ni–L1 (green). Experimental: mw frequency 9.432 GHz, mod. ampl. 1 mT, mw power 10 mW. Asterisk: a resonator signal. Left: structures of Ni–C and Ni–L for standard hydrogenases.

Protons related to the H_2 oxidation process can be ($^1H/^2H$) exchanged and thus uniquely identified.[9–12] Electron-nuclear double resonance (ENDOR) and hyperfine sublevel correlation (HYSCORE) spectroscopies can be employed, as these methods are sensitive to hyperfine interactions of magnetic nuclei such as ^1H or ^2H. Such a study proved to be very challenging for Hase I due to several system-related drawbacks (ESI‡). In this work Ni–C is characterized by FTIR, CW EPR, HYSCORE and ENDOR in protonated/deuterated samples.

[a] *Max-Planck-Institut für Bioanorganische Chemie, Stiftstr. 34-36, 45470 Mülheim/Ruhr, Germany. E-mail: wolfgang.lubitz@mpi-mail.mpg.de*
[b] *Laboratoire de Bioénergétique et Ingénierie des Protéines, IMM-CNRS, 13402, Marseille, France. E-mail: giudici@ifr88.cnrs-mrs.fr*
[c] *Max-Planck-Institut für Dynamik komplexer technischer Systeme, Sandtorstr. 1, 39106 Magdeburg, Germany. E-mail: matthias.stein@mpi-magdeburg.mpg.de*

† This article is part of the *ChemComm* 'Artificial photosynthesis' web themed issue.

‡ Electronic supplementary information (ESI) available. See DOI: 10.1039/c1cc16109a

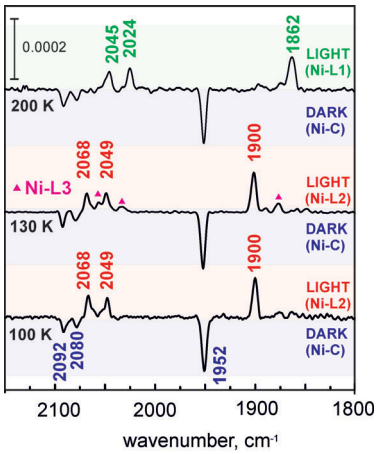

Fig. 2 Light-minus-dark FTIR spectra recorded at cryogenic temperatures. In FTIR, additional light-induced states (*e.g.* Ni–L3) could be resolved. Averages: 4000 scans, resolution: 2 cm^{-1}.

DFT calculations complement and support spectral simulations and assignments.

Reduction of Hase I with H_2 results in the formation of a paramagnetic state with principal *g*-values $g_x = 2.21$, $g_y = 2.15$ and $g_z = 2.01$ (Fig. 1), which resembles the Ni–C from mesophilic hydrogenases.[9,10] The g_x, g_y values are however slightly up-shifted indicating a somewhat different electronic structure. This state is associated with a formally trivalent Ni(III) species with the unpaired electron in a d_{z^2} orbital.[13]

Heterolytic splitting of H_2 results in the formation of a bridging hydride in the active site of Ni–C, as illustrated in Fig. 1. Illumination at low temperatures converts Ni–C to the Ni–L state(s),[14] in which photodissociation of the hydride as a proton takes place,[12,15] leaving the nickel ion in a formal Ni(I) state.[13,14] This is shown also for the Ni–C state in Hase I by the formation of two light-induced states Ni–L1 and Ni–L2 after illumination at 170 K and 100 K, respectively. Unlike O_2-sensitive hydrogenases, Ni–L1 is, however, also observed at $\leq$100 K even in the absence of light.[16] On the other hand, the IR stretching frequencies measured for the Ni–C and Ni–L states are within the range of those reported for standard hydrogenases (Fig. 2),[15] suggesting a similar charge density on the Fe ion.

The deuterated form of Ni–C was prepared by reducing the enzyme with $^2H_2$ in a ^2H_2O-based buffer. The HYSCORE spectra obtained at the principal positions g_x and g_y are shown in Fig. 3. In these spectra, correlations between nuclear frequencies of different electronic manifolds corresponding to ^{14}N and ^2H nuclei are present. The ^{14}N signals (Fig. 3) belong to the N_ε nitrogen of a histidine that is hydrogen bonded to a bridging cysteine with quadrupole and hyperfine coupling values in very good agreement with those reported for mesophilic hydrogenases.[7,17,18]

In the HYSCORE spectra shown in Fig. 3 a ridge centred at the ^2H Larmor frequency is also observed, showing the presence of at least one ($^1H/^2H$) exchangeable proton in the [NiFe] site of Ni–C. The g_z orientation is not shown, since at this field position contributions from exchangeable protons originating from the iron–sulfur centers are present. At the Q-band the ^2H ridge in the g_y orientation is clearly detectable, with no overlap of the ^{14}N signals (Fig. 3C). Illumination at

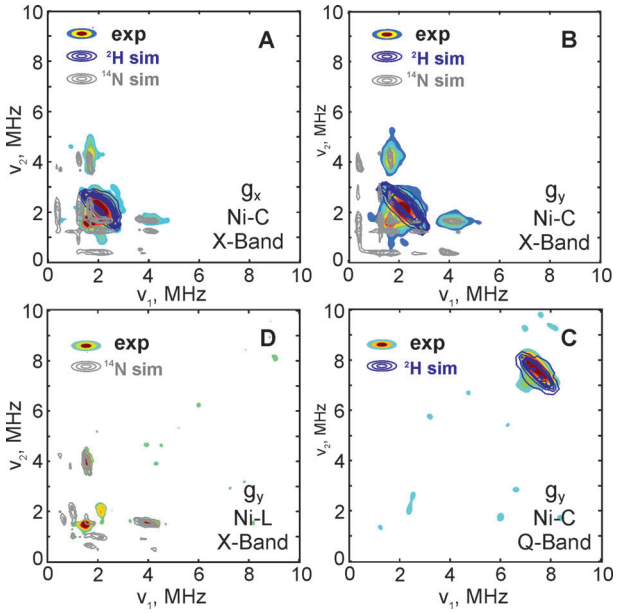

Fig. 3 (A, B, C) X- and Q-band HYSCORE of Ni–C prepared in ^2H_2O ($^2H_2$) at g_x, g_y orientations. The simulated spectra of the ^{14}N and ^2H signals have been overlaid. For details refer to ESI.‡ ^2H simulation parameters were obtained from the ENDOR experiments (Fig. 4). (D) Illumination converts Ni–C to Ni–L2 with concomitant loss of ^2H ridges of the deuterated form of the hydride.

7 K converts the Ni–C to Ni–L2. The HYSCORE spectrum recorded at the g_y (323.6 mT) position shows that the ridges associated with the exchangeable proton are absent in Ni–L2. Instead, only a small isotropic signal centered at the Larmor frequency of 2.11 MHz is observed (Fig. 3D). Similar results were found for other orientations. The ^2H ridges can be thus associated with the deuterated form of the hydride ligand present in the Ni–C state of Hase I, which is dissociated upon illumination[9,10,12] (Fig. 1).

To further characterize the ($^1H/^2H$) exchangeable protons bound to the Ni–C state, a ^2H Mims ENDOR study at Q-band frequency was carried out. At Q-band the nuclear frequencies of ^{14}N and ^2H are well separated and Mims ENDOR can resolve small hyperfine interactions of ^2H nuclei.[11] The EPR spectrum of the Ni–C state showed a small splitting of the Ni signals due to the magnetic interaction with the reduced proximal [FeS] cluster[8] (ESI‡). The ENDOR spectra shown in Fig. 4 were recorded for field positions close to g_x (1106.1 mT) and down to the lowest *g*-value ($g = 2.10$), at which contributions from the iron–sulfur centres are negligible. In these spectra, only signals related to exchangeable protons in the local surrounding of the spin carrying [NiFe] site in Ni–C are present.

Two hyperfine couplings were determined corresponding to two distinct deuterons; $^2H(1)$ and $^2H(2)$. The coupling of $^2H(1)$ is relatively large and anisotropic with principal components $A_{x,y,z} = (+1.95, -0.95, -1.8) \pm 0.15$ MHz (Fig. 4, red shaded line). Using these parameters, the ^2H ridges in the HYSCORE spectra could be very well simulated. The isotropic part ($A_{iso} = -0.27 \pm 0.15$ MHz) is small, which would be in line with a rather remote ligand of nickel in the equatorial plane of the d_{z^2} orbital.[11] Thus, this coupling can be assigned to the deuterated hydride ($^2H^-$) in the Ni–C state. The magnitudes of the dipolar

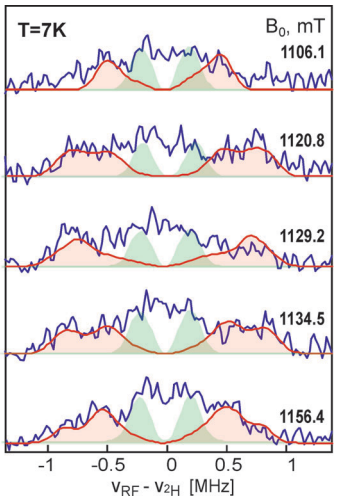

Fig. 4 ^{2}H Mims ENDOR spectra. The simulation of the coupling of the deuteride ligand ^{2}H(1) is shown in red and of the second coupling ^{2}H(2) in green. Experimental: $\pi/2$ = 36 ns, rf = 33 μs, mw frequency = 33.99 GHz, T = 7 K. Accumulation time: between 48 and 72 hours.

and isotropic components are significantly smaller compared to those found in *Desulfovibrio vulgaris* Miyazaki F[10] and the regulatory enzyme from *Ralstonia eutropha* with $A_{x,y,z}$ = (+2.8, −1.7, −2.8 MHz), A_{iso} = −0.54 MHz);[9] this suggests a larger bonding distance and a weakening of the interaction of the hydride in the active site of Ni–C in Hase I. The second coupling ^{2}H(2) is rather small and isotropic ≤0.5 MHz. A similar signal was reported for Ni–C in *D. gigas*, where it was associated with a ^2H_2O molecule.[11] At present, no definitive assignment for this coupling is possible. The accurate determination of the ^{2}H(1) exchangeable hydron hyperfine tensor orientation is limited by the signal-to-noise ratio and the restricted field-dependent study. On the basis of the Ni–C EPR spectrum a molecular structure similar to the [NiFe] site of the *D. vulgaris* MF enzyme is proposed, for which the *g*-tensor has been determined.[19] The most likely assignment is that with the largest ^{1}H dipolar component A'_x of +14 MHz (A_{1H}/A_{2H} = 6.514), which points approximately along the g_x direction (26°). Assuming that the point-dipole approximation is valid and considering a spin density at the Ni of ρ = 0.6,[13] an elongated distance of 1.86 Å for the Ni–H bond can be inferred, while for *D. vulgaris* MF the same approximation yielded an estimated distance of 1.60 Å (A'_x = +21.9 MHz).[10] DFT calculations on geometry optimized models of Ni–C showed a good agreement for the calculated *g*-tensor values and hyperfine coupling parameters of the bridging hydride (A'_x(DFT) = +12.6 MHz) (see ESI‡). In these calculations a systematic upshift of the *g*-values and a decrease in the hyperfine coupling values of the hydride correlate with an increase in the Ni–H bond distance from approximately 1.6 Å in standard hydrogenases to approximately 1.8 Å in Hase I. Second order contribution to the hyperfine interaction (spin–orbit coupling) plays a significant role in short Ni–H distances and accounts for 10–20% of the hfc.

The EPR spectrum of Ni–C in Hase I suggests a molecular symmetry of the [NiFe] site similar to that of O_2-sensitive hydrogenases. A light-sensitive hydride ligand coordinates the active site of Ni–C that is, however, more weakly bound than that in *D. vulgaris* MF and *R. eutropha* (RH) enzymes (by 2.5 kcal mol^{-1} at the BP86 and 3.8 kcal mol^{-1} at the B3LYP + D level). The smaller hyperfine interaction can be associated with an increased bond distance between the nickel and the hydride and a more asymmetric bridging situation between Ni and Fe.[20] Slight geometrical changes in the first and second coordination sphere of the nickel ion, basicity of proton acceptors, and/or hydrogen bonding interactions can affect the pK_a of the metal hydride complex and may result in weakening of the Ni–H bond.[21,22] The weaker binding of the hydride found in the present work is in line with the increased light sensitivity of Ni–C, the decreased stability and the more positive catalytic potential of the hydride complex observed in IR electrochemical titrations[6] and the transition to a non-conventional Ni–R state (suggested to be unprotonated).[6] The weaker Ni–H bond might also be of relevance in the bias of O_2-tolerant enzymes towards H_2 oxidation (more acidic nickel hydride), as has been shown similarly for biomimetic compounds.[20,22]

Work has been supported by SOLAR-H_2, and Région Provence-Alpes-Côte d'Azur. Simulations were performed with the program *KAZAN* developed by A. Silakov and B. Epel.

Notes and references

1 P. M. Vignais, B. Billoud and J. Meyer, *FEMS Microbiol. Rev.*, 2001, **25**, 455–501.
2 B. E. Barton, M. T. Olsen and T. B. Rauchfuss, *Curr. Opin. Biotechnol.*, 2010, **21**, 292–297.
3 M. Guiral, P. Tron, V. Belle, C. Aubert, C. Léger, B. Guigliarelli and M. T. Giudici-Orticoni, *Int. J. Hydrogen Energy*, 2006, **31**, 1424–1431.
4 X. J. Luo, M. Brugna, P. Tron-Infossi, M. T. Giudici-Orticoni and E. Lojou, *JBIC, J. Biol. Inorg. Chem.*, 2009, **14**, 1275–1288.
5 M. Brugna-Guiral, P. Tron, W. Nitschke, K. O. Stetter, B. Burlat, B. Guigliarelli, M. Bruschi and M. T. Giudici-Orticoni, *Extremophiles*, 2003, **7**, 145–157.
6 M. E. Pandelia, V. Fourmond, P. Tron-Infossi, E. Lojou, P. Bertrand, C. Léger, M. T. Giudici-Orticoni and W. Lubitz, *J. Am. Chem. Soc.*, 2010, **132**, 6991–7004.
7 W. Lubitz, E. Reijerse and M. van Gastel, *Chem. Rev.*, 2007, **107**, 4331–4365.
8 M. E. Pandelia, W. Nitschke, P. Infossi, M. T. Giudici-Orticoni, E. Bill and W. Lubitz, *Proc. Natl. Acad. Sci. U. S. A.*, 2011, **108**, 6097–6102.
9 M. Brecht, M. van Gastel, T. Buhrke, B. Friedrich and W. Lubitz, *J. Am. Chem. Soc.*, 2003, **125**, 13075–13083.
10 S. Foerster, M. van Gastel, M. Brecht and W. Lubitz, *JBIC, J. Biol. Inorg. Chem.*, 2005, **10**, 51–62.
11 C. L. Fan, M. Teixeira, J. Moura, I. Moura, B. H. Huynh, J. Legall, H. D. Peck and B. M. Hoffman, *J. Am. Chem. Soc.*, 1991, **113**, 20–24.
12 J. P. Whitehead, R. J. Gurbiel, C. Bagyinka, B. M. Hoffman and M. J. Maroney, *J. Am. Chem. Soc.*, 1993, **115**, 5629–5635.
13 M. Stein and W. Lubitz, *Phys. Chem. Chem. Phys.*, 2001, **3**, 5115–5120.
14 J. W. van der Zwaan, S. P. J. Albracht, R. D. Fontijn and E. C. Slater, *FEBS Lett.*, 1985, **179**, 271–277.
15 P. Kellers, M. E. Pandelia, L. J. Currell, H. Görner and W. Lubitz, *Phys. Chem. Chem. Phys.*, 2009, **11**, 8680–8683.
16 K. Knüttel, K. Schneider, A. Erkens, W. Plass, A. Müller, E. Bill and A. X. Trautwein, *Bull. Pol. Acad. Sci., Chem.*, 1994, **42**, 495–511.
17 A. G. Agrawal, M. van Gastel, W. Gärtner and W. Lubitz, *J. Phys. Chem. B*, 2006, **110**, 8142–8150.
18 A. Chapman, R. Cammack, C. E. Hatchikian, J. McCracken and J. Peisach, *FEBS Lett.*, 1988, **242**, 134–138.
19 S. Foerster, M. Stein, M. Brecht, H. Ogata, Y. Higuchi and W. Lubitz, *J. Am. Chem. Soc.*, 2003, **125**, 83–93.
20 B. E. Barton and T. B. Rauchfuss, *J. Am. Chem. Soc.*, 2010, **132**, 14877–14885.
21 M. R. Dubois and D. L. Dubois, *Chem. Soc. Rev.*, 2009, **38**, 62–72.
22 Y. A. Small, D. L. Dubois, E. Fujita and J. T. Muckerman, *Energy Environ. Sci.*, 2011, **4**, 3008–3020.